Dalton Transactions

Accepted Manuscript

ROYAL SOCIETY OF CHEMISTRY

www.rsc.org/dalton

Title: Analysis of Trivalent Cation Complexation to Functionalized Mesoporous Silica using Solid-State NMR Spectroscopy

Authors: Jennifer Shusterman[†], Harris Mason[‡], Anthony Bruchet[†], Mavrik Zavarin[‡], Annie B. Kersting[‡], and Heino Nitsche[†]

Manuscript ID: DT-ART-08-2014-002380

Table of Contents Entry:

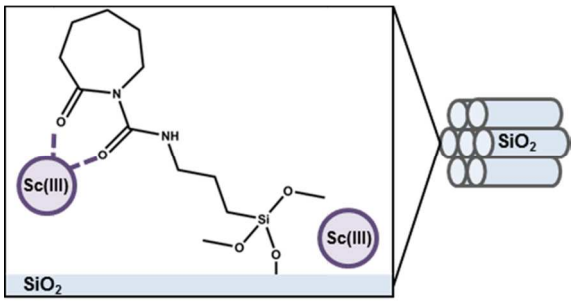

The first comprehensive study of Al(III) and Sc(III) interactions with a novel hybrid material, N-[5-(trimethoxysilyl)-2-aza-1-oxopentyl]caprolactam functionalized mesoporous silica, was conducted using solid-state NMR spectroscopy.

Analysis of Trivalent Cation Complexation to Functionalized Mesoporous Silica using Solid-State NMR Spectroscopy

Jennifer Shusterman[†], Harris Mason[‡], Anthony Bruchet[†], Mavrik Zavarin[‡], Annie B. Kersting[‡], and Heino Nitsche[†,*]

[†]Department of Chemistry, University of California, Berkeley; Berkeley, California, 94720.

[‡]Glenn T. Seaborg Institute, Physical and Life Sciences Directorate, Lawrence Livermore National Laboratory, L-231, PO Box 808, Livermore, California, 94550.

*Deceased

ABSTRACT

Functionalized mesoporous silica has applications in separations science, catalysis, and sensors. In this work, we studied the fundamental interactions of trivalent cations with functionalized mesoporous silica. We contacted trivalent cations of varying ionic radii with N-[5-(trimethoxysilyl)-2-aza-1-oxopentyl]caprolactam functionalized mesoporous silica with the aim of probing the binding mechanism of the metal to the surface of the solid. We studied the functionalized silica using solid-state nuclear magnetic resonance (NMR) spectroscopy before and after contact with the metals of interest. We collected NMR spectra of the various metals, as well as of ^{29}Si and ^{13}C to probe the silica substrate and the ligand properties, respectively. The NMR spectra indicate that the metals bind to the functionalized silica via two mechanisms. Aluminum sorbed to both the silica and the ligand, but with different coordination for each. Scandium also sorbed to both the silica and the ligand, and unlike the aluminum, had the same coordination number. Additionally, the functionalized silica was susceptible to acid hydrolysis and two primary mechanisms of degradation were observed: detachment from the silica surface and opening of the seven-membered ring in the ligand. Opening of the seven-membered ring may be beneficial in that it decreases steric hindrance of the molecule for binding.

INTRODUCTION

Development of high-capacity solid-phase materials that selectively complex metals is necessary for the advancement of chromatography resins, catalysts, sensors, and separation schemes for the treatment of spent nuclear fuel. Currently, many large-scale metal separation techniques utilize liquid-liquid separations. Liquid-liquid separations have the major disadvantage that they generate large volumes of hazardous organic waste. By grafting selective ligands to the surface of a chemically robust high surface area solid support, selective and efficient solid-phase metal extractants could be developed. Use of these materials for metal extractions would

reduce the production of hazardous organic waste and they could then be used to remove metals directly from mineral acids. Additionally, by immobilizing ligands to solid supports, solid-phase metal extractants and solid catalysts could be produced with the benefit of reusability.

While ligands have been grafted to silica for catalytic applications in the past, there has been minimal characterization of the metal complexes formed.[1–3] There has been one X-ray absorption spectroscopy study of the metal[4] and nuclear magnetic resonance (NMR) spectroscopy studies characterizing the ligands bound to metals[5,6], but no direct NMR characterization of the metals has been reported. The research presented here is broadly aimed at understanding metal interactions with organically modified solid supports. By determining how metals interact with these materials, improvements can be made in the development of separation and catalyst materials.

This work focuses on organically-modified SBA-15 type mesoporous silica. SBA-15 type mesoporous silica was chosen for this work because of its high surface area, chemical stability, tunable pore and particle size.[7] By covalently bonding selective ligands to the surface of SBA-15, enhanced chemical stability and metal capacity is expected relative to solid-phase metal extractants made by coating ligands on polymer or silica supports. The ligand chosen for this work is a derivative of a carbamoyl acetamide (CA), and is expected to be selective towards trivalent cations with large ionic radii (>0.9 Å). This ligand was selected because of its similarity to a malonamide, which has been shown to successfully complex trivalent lanthanides for nuclear fuel cycle application.[8–16] We tested two smaller trivalent cations, Al (0.39-0.535 Å) and Sc (0.745-0.870 Å),[17] to determine if their ionic radius would impact how they bind to the functionalized mesoporous silica.

Earlier work on functionalized mesoporous silica focused mainly on the metal sorption experiments as opposed to the binding mechanisms allowing for selectivity.[18–23] Additionally, the extent of degradation of functionalized mesoporous silica was not thoroughly studied, which raises the question of whether the ligands decomposed after acid contact. The goal of this work is to elucidate the fundamental interactions of two trivalent cations with a CA-functionalized mesoporous silica using NMR spectroscopy. By using various NMR spectroscopic techniques, a more thorough understanding of these interactions is possible. In this work, we

probed the metal, surface, and ligand nuclei to create a detailed picture of the chemistry involved with this system. Despite the relatively large number of publications studying metal uptake on functionalized silica, NMR has not been used to probe these metals directly. NMR has been used to probe metals in organometallic crystals and in mineral environments of these same metals,[24–30] but the work presented here is the first to examine the binding mechanism of the metal to functionalized mesoporous silica using NMR of the metal nuclei.

We studied the binding behavior of two trivalent cations, Al and Sc to investigate the effect of cation size on metal complexation. We performed all studies at low pH to ensure that hydrolysis products of the metals were not present. The cations were chosen as representative metals because their NMR-active nuclei ^{27}Al and ^{45}Sc are 100% naturally abundant, and easily observed directly. Additionally, the ligand and surface properties were examined using ^{13}C and ^{29}Si NMR, respectively, to determine if changes to either the ligand or surface would be evident upon complexation with a metal.

EXPERIMENTAL METHODS

Material Preparation

Our method for synthesis of spherical particle SBA-15 type mesoporous silica with 8 nm pore diameter was adapted from Katiyar et al.[31] The "CA" ligand, N-[5-(trimethoxysilyl)-2-aza-1-oxopentyl]caprolactam (Gelest), was grafted to the silica surface via toluene reflux using the method of Fryxell[19] (Figure 1a). Methanol, water, and a small fraction of the toluene were distilled at the end of the condensation. The functionalized silica (pristine solid) was filtered, washed with 2-propanol, and air-dried. Final ligand density on the surface was 0.59 molecules per nm^2 as measured by thermogravimetric analysis (TGA).

Batch Sorption Experiments

Stock solutions of 70 mM were prepared from the aluminum and scandium nitrate salts. Stock solutions had pH values between 2.5 and 3.8. In polypropylene centrifuge cones, 40 mg of solid (either bare SBA-15 with 8 nm pores or SBA-15 functionalized with the CA ligand) was combined with 11 mL of ultrapure water (18.0 MΩ˙cm) and , if necessary, acidified with 0.1 M nitric acid until the pH was less than 5.5. Samples were shaken and left to

pre-equilibrate for approximately 24 hours. After 24 hours, 1 mL of the appropriate metal nitrate stock solution was added to the pre-equilibrated samples and acidified to pH 3.0 with 0.1 M nitric acid. The total metal ion concentration was approximately 6 mM. Aliquots were removed from the supernatant of the samples every few hours for solution-state NMR spectroscopy analysis. After 24 hours from the time of metal addition, the solid was collected from the sample via suction filtration through a 0.22 μm filter, washed with ethanol, and allowed to air dry overnight. A control sample was made by combining 40 mg of the CA functionalized silica with 12 mL of pH 3 nitric acid, contacting for 24 hours, and collecting the solid via suction filtration. An additional desorption on the Al-CA-SBA and Sc-CA-SBA samples was performed by contacting the solid with Milli-Q water for 10 minutes prior to collecting the solid via suction filtration, washing with water then ethanol, and drying overnight.

NMR spectroscopy.

The bulk of the NMR spectra were collected on a 300 MHz (7.5 T) Tecmag Apollo using a Bruker HX CP/MAS probe configured for 4 mm (o.d.) rotors. A $^{29}Si\{^{1}H\}$ single pulse magic angle spinning (SP/MAS) spectrum was collected on the pristine solid at a spinning rate of 10 kHz with a pulse delay of 120 s. The $^{29}Si\{^{1}H\}$ cross-polarization magic angle spinning (CP/MAS) NMR spectra were collected on solid samples at a spinning rate of 10 KHz using 3 ms continuous wave (CW) polarization transfer and a 2 s pulse delay. The $^{13}C\{^{1}H\}$ CP/MAS NMR spectra were collected at a spinning rate of 10 kHz and used a 1 ms ramped amplitude polarization transfer on the ^{13}C channel, CW decoupling on the ^{1}H channel during acquisition, and a 2 s pulse delay. Operating frequencies were 59.82, 75.73, and 301.13 MHz for ^{29}Si, ^{13}C, and ^{1}H, respectively, and spectra were referenced in each case to tetramethylsilane (TMS). While not inherently quantitative, the CP/MAS spectra can be compared between samples as they were collected under identical conditions for each respective nucleus. Additionally, it is not expected that the CP kinetics will change due to reactions presented in this manuscript. ^{27}Al and ^{45}Sc NMR were performed at operating frequencies of 78.46 and 73.15 MHz for ^{27}Al and ^{45}Sc, respectively. For aliquots of supernatant solutions, 14.5 and 15.5 μs pulse widths (corresponding to a 90° tip angle) with recycle delays of 0.5 and 0.2 s were used for ^{27}Al and ^{45}Sc, respectively. To maintain consistency between measurements, the same

volume (65 uL) of solution was added to the 4 mm (o.d.) ZrO_2 rotor for each sample. The integrated peak intensity for each sample was compared to that of a blank. The blank was prepared by combining 1 mL of the 70 mM metal nitrate stock solution with 11 mL of ultrapure water and acidifying to pH 3 with 0.1 M nitric acid. The ^{27}Al and ^{45}Sc single pulse MAS spectra of solid samples were performed with same probe head using a spinning rate of 10 kHz, and a pulse delay of 0.5 and 0.2 s for ^{27}Al and ^{45}Sc, respectively. Additionally, ^{45}Sc single pulse MAS spectra of the solid samples were collected on a 500 MHz Bruker Avance spectrometer with a DOTY probe. These were collected while spinning at 10 kHz with a pulse delay of 0.2 s. The spectra collected on the 500 MHz spectrometer are presented in the supporting information. In each case short, 1 µs pulses were used to ensure that quantitative results could be obtained and correspond to 6.2° and 5.8° tip angles for ^{27}Al and ^{45}Sc, respectively. The ^{27}Al and ^{45}Sc spectra were referenced to their respective 70 mM metal nitrate stock solution (δ_{Al}=0.0 ppm and δ_{Sc}=0.0 ppm). All spectra were analyzed by fitting the peaks to pseudo-Voigt functions to obtain integrated intensity and the chemical shift.

The $^{1}H\{^{45}Sc\}$ Transfer of Populations in Double Resonance (TRAPDOR) [32,33] and ^{1}H Double Quantum (DQ) correlation experiments were collected with a MAS rate of 50 kHz on a 600 MHz Avance III spectrometer equipped with a Bruker Very Fast MAS probe configured for 1.3 mm o.d. rotors. The $^{1}H\{^{45}Sc\}$ TRAPDOR experiment was collected as a set of two spectra where a spin-echo control spectrum (S_0) was collected in the absence of ^{45}Sc irradiation, and a TRAPDOR spectrum (S) was collected where the ^{45}Sc channel was irradiated with a 100 kHz dephasing pulse for 16 acquisitions each and a 10 s pulse delay using a 4.6 ms dephasing period (230 rotor cycles). The ^{1}H DQ correlation experiment was collected using the Back to Back (BaBa) sequence.[34,35] A total of 128 spectra were collected in t_1 using the States-TPPI method for 64 acquisitions each at a 20 µs increment corresponding to a spectral width of 50 kHz in the indirect dimension. ^{1}H spectra were all referenced to an external standard of hydroxylapatite by setting the hydroxyl resonance to δ_H = 0.2 ppm[36].

RESULTS

Pre-conditioned solid

Very few studies have examined the degradation of organically modified silica in the presence of acid. The state of the functional layer of the silica after contact with acid is important, as it impacts the binding mechanism with metals of interest as well as the lifetime of the material. A previous study on organically modified silica has indicated slight degradation of these materials at the silane anchor in the presence of acid.[37] We used the results from ^{29}Si and ^{13}C NMR spectroscopy to investigate the mechanism of degradation for CA functionalized SBA-15 in the presence of nitric acid. The ^{29}Si{^{1}H} CP/MAS NMR (Figure 2b) and ^{13}C{^{1}H} CP/MAS NMR (Figure 3b) were performed on the solid recovered after 24 hours of contact with pH 3 nitric acid (pre-conditioned solid) and compared to the pristine functionalized material (Figures 2a and 3a, respectively). This experiment was done to determine the extent of ligand degradation from pH 3 nitric acid prior to metal contact. In the ^{29}Si{^{1}H} CP/MAS NMR spectrum, there are two groups of peaks: Q (δ_{Si}= -92 to -112 ppm) and T (δ_{Si}= -50 to -70 ppm) peaks, the latter being silicon atoms bound to the ligand. Q^n and T^m peaks are defined as $Si(OSi)_n(OH)_{4-n}$ and $SiR(OSi)_m(OH)_{3-m}$, respectively, where R is a carbon chain. In the ^{29}Si{^{1}H} CP/MAS NMR spectrum of the pre-conditioned sample, some T peaks remain and indicate that the acid treatment did not completely degrade the ligand-silane anchor (Figure 2b). As the CP/MAS NMR spectra for the pristine and pre-conditioned samples were collected under identical condition, the relative ratios of T^1 and T^2 can be compared to determine the relative change in concentration of each of these species. This method was used as opposed to quantifying the T peaks of a single-pulse (SP) experiment due to the minimal ligand surface coverage, resulting in very low T peak intensity even after multiple days of collection (SI, Figure S1). The ratio of T^1 (δ_{Si} = -51 ppm) to T^2 (δ_{Si} = -58 ppm)[38] is lower (T^1:T^2 is 4.1 and 0.36 for pristine and preconditioned, respectively) than the pristine solid prior to contact with acid. The decrease in T^1 is not surprising as a T^1 linkage to the surface is the most hydrolysable of T^1, T^2, and T^3. However the extent of hydrolysis was more than expected at approximately 90% loss of T^1 peak intensity, correlating to approximately the same loss in T^1 species on the surface under the aforementioned identical collection conditions. Specifically, the T^1 species that hydrolyze are converted to Q^3 species. The ^{13}C{^{1}H} CP/MAS NMR spectra look similar before and after contact with the pH 3 nitric acid, however, the peak at 48 ppm decreases significantly after acid contact causing corresponding changes in peak intensities for the other –CH_2

groups. This peak is assigned to the carbon directly bound to the nitrogen in the seven-membered ring. The decrease in the peak indicates that the ring opened in the presence of acid (Figure 1b). There is an increase in intensity at 7 ppm resonance, which is indicative of the terminal $-CH_3$ produced by the opening of the ring.

Metal Interactions with Bare SBA-15

To understand the behavior of Al(III) and Sc(III) on functionalized SBA-15, we first characterized the interactions of these metals with the bare SBA-15 surface. As the silica surface may not be coated in a perfect monolayer of ligand based on the surface coverage compared to literature values,[19] there are gaps between the ligand molecules in which the metals can interact with the silica surface. The $^{29}Si\{^1H\}$ CP/MAS NMR spectrum (SI, Figure S2a) of Al on SBA-15 (Al-SBA) indicated the presence of Q^4, Q^3, and Q^2 surface species. The relative ratios of each of the Q peaks indicate that the Q^3 sites are the most prevalent surface species, which is expected in an unfunctionalized silica material at this pH. The substitution of Al for a Si in the SBA-15 would result in a chemical shift of between δ_{Si} =-97 and δ_{Si} =-107 ppm,[39] and would overlap with the Q^3 peak centered at δ_{Si} =-102 ppm. Based on the small amount of Al on the surface relative to the total number of surface Si sites, it is unlikely that any change in the $^{29}Si\{^1H\}$ CP/MAS NMR spectrum would be observed from the pre-conditioned sample compared to the Al-contacted sample.[25] Similar reasoning follows for why we would not expect to see a change in the $^{29}Si\{^1H\}$ CP/MAS NMR spectrum for the Sc sorption on SBA-15 (Sc-SBA). The $^{29}Si\{^1H\}$ CP/MAS NMR spectrum (SI, Figure S2b) of the Sc-SBA also contained Q^4, Q^3, and Q^2 peaks and is similar to that collected for Al-SBA. The Al-SBA and Sc-SBA spectra do not differ significantly from one another or from acid treated silica that has not been contact with a metal, following the expected behavior for low metal coverage.

The ^{27}Al SP/MAS NMR spectrum of Al-SBA (Figure 4a) has a broad asymmetric peak with a peak maximum at approximately δ_{Al} = 50 ppm and corresponds to Al in tetrahedral coordination. This result agrees with the literature where Al was found to bind to the silanol groups on the silica surface in bidentate tetrahedral complexes.[24,25] As noted by Houston,[25] the width of this peak is indicative of a motion-constrained species which supports a bidentate complex to the silica surface. The Al here is binding to the deprotonated silanol groups on the silica surface forming an inner sphere complex. Additionally, a sharp peak near δ_{Al} =0 ppm is indicative of

187 $Al(H_2O)_6^{3+}$ trapped in the pores of the silica. Nevertheless, approximately 88% of the Al bound to the solid had a
188 coordination number of 4 and was bound as an inner sphere complex to the surface.

189 The ^{45}Sc SP/MAS NMR spectrum (Figure 5a) of the Sc-SBA has a single, asymmetric peak with a peak
190 maximum at about δ_{Sc} = 46 ppm and corresponds to that typical for a Sc coordination number of seven. The 7-
191 coordinated Sc observed here is unexpected given the well-ordered surface structure of the SBA-15. In well-
192 ordered environments Sc typical adopts a coordination of 6 or 8[29,40–42], but a 7-coordinated Sc is more typical of
193 a disordered local environment.[27,28,41–43] Additionally, in aqueous systems at pH 3.5, Sc has been found to be
194 most stable in a 7-coordinate complex.[41] The Sc has been assigned this coordination, however, due to the
195 measured chemical shift which is in the range expected for 7-coordinated species and far from the expected
196 chemical shifts of both the 6 and 8-coordinated species.[28] Unlike the Al-SBA solid spectrum, no peak
197 corresponding to aqueous $Sc(NO_3)_3$ was observed . We have not been able to identify what may cause retention
198 of the aqueous metal salt in some samples but not others.

199

200 *Metal Interaction with CA-SBA*

201 The interactions of Al(III) and Sc(III) as model trivalent cations with CA functionalized SBA (CA-SBA) were
202 examined by analyzing the solutions and solids after metal sorption. Initial analysis of these solids by ^{29}Si and ^{13}C
203 NMR indicate that the same mechanism of CA ligand degradation observed for the preconditioned solid occurs
204 in these systems as well (Figures 6 and 7). Insight into the binding of Al and Sc to the CA-SBA was gained from
205 the direct observation of the local Al and Sc environments using ^{27}Al and ^{45}Sc NMR spectroscopy, respectively.
206 The solution ^{27}Al NMR measurements of the aqueous aliquots removed during the Al sorption experiments
207 indicated that approximately 35% of the Al is bound to the functionalized silica surface after one day of metal
208 contact time (SI, Figure S3). An analogous measurement of ^{45}Sc on the solution phase from the Sc sorption
209 experiment indicated that approximately 49% of the Sc in solution sorbed to the solid (SI, Figure S4). While the
210 resonance in the solution phase of the Sc sorption experiment was shifted by -1 ppm relative to the Sc blank,
211 the sorption can still be determined from the integrated peak intensity, as the shift only indicates a change in

local environment for the Sc. Based on the post-functionalization surface area of the CA-SBA material and the initial 6 mM Al and Sc concentrations for each of these samples, the metal ion coverages were 1.3 and 1.8 μmol/m^2 for Al and Sc, respectively.

The ^{27}Al SP/MAS NMR spectrum (Figure 4b) of aluminum sorbed to the CA-SBA-15 (Al-CA-SBA) contains two distinct peaks with peak maxima at δ_{Al} = 10 ppm and δ_{Al} = 48.5 ppm that correspond to Al in octahedral and tetrahedral coordination, respectively. Additionally, there is a sharp peak at δ_{Al} = 0 ppm that is due to aqueous $Al(H_2O)_6^{3+}$ trapped in the pore structure, such as observed in the Al-SBA sample. Based on the Al-SBA results, the tetrahedral Al is again assigned to Al sorbed directly to the silica surface. Given its absence in the Al-SBA sample, the octahedral Al represents complexation with the ligand carbonyls. About 46% of the sorbed Al is 4-coordinate compared to the 88% observed for the Al-SBA sample and 49% is now represented by a 6-coordinate species. The remaining 12% and 5% of Al in the Al-SBA and Al-CA-SBA, respectively, are from the $Al(H_2O)_6^{3+}$ species. If the aluminum had precipitated as a hydroxide, the chemical shift would be higher than that assigned to the octahedral peaks.[44] Additionally, the concentration and pH used for these studies limits Al-hydroxide formation.[24] Based on this spectrum and the total amount of sorbed Al, a 1:1 metal ligand coordination for the octahedral Al is likely with the remaining space in the coordination sphere occupied by water molecules.

A desorption experiment was performed on the Al-CA-SBA solid to determine the reversibility of the sorption reactions. The ^{27}Al SP/MAS NMR spectrum collected of the desorbed sample (Figure 8) indicates a near complete loss of the peaks that had been present prior to water contact to the point where instrument noise overwhelms any ^{27}Al signal. The lack of Al signal in this sample indicates that brief contact (10 min) with water was sufficient to desorb the Al. Based on Al speciation,[24] we expect that at the pH of Milli Q water, Al precipitates as $Al(OH)_3$ which is subsequently washed off of the surface. This result indicates that the Al sorption is reversible which is necessary for any materials used with chromatographic applications.

The ^{45}Sc SP/MAS NMR spectrum (Figure 5b) of the Sc sorbed onto the CA functionalized silica (Sc-CA-SBA) has a single, broad asymmetric peak with the peak maximum located at approximately δ_{Sc} = 36 ppm and again corresponds to that expected for a 7-coordinated Sc species.[28,45] We postulate that the Sc could adopt a

distorted capped trigonal prism geometry similar to that proposed before for Sc compounds with bidentate oxygen-donor ligands.[27] In the spectrum collected on the 300 MHz spectrometer, the broad peak could encompass a small shoulder centered at δ_{Sc} =-20 ppm, corresponding to 8-coordinated Sc. To determine whether a resonance at δ_{Sc} =-20 ppm was present or whether the broadening of the peak to this range of chemical shifts was due to the impact of the ligands on the electric field gradient, we measured the sample on a 500 MHz spectrometer (SI, Figures S5, S6). In this spectrum, it is clear that there is no peak at that chemical shift, and thus the presence of 8-coordinated Sc has been ruled out. Despite Sc having the same coordination number for both the Sc-SBA and the Sc-CA-SBA samples, the spectra were still unique in that the Sc-CA-SBA has a much broader peak indicating a change in local coordination environment for the Sc nuclei in the Sc-CA-SBA sample. As the only difference between these two samples is the presence of the CA ligand in the Sc-CA-SBA sample, we assign this difference in coordination environment to Sc interacting with the CA ligand.

To further probe the Sc interactions with the CA-SBA material, ^{1}H spectra were collected for both the pre-conditioned (Figure 9a) and the Sc-CA-SBA (Figure 9b) samples. In comparing these two spectra, a peak unique to the Sc-CA-SBA sample is observed at 4.3 ppm that we attribute to the presence of inner sphere waters on the Sc ion. This water is associated with Sc and not simply relic physisorbed water on the bare surface as evidenced by the lack of a peak at this chemical shift for the preconditioned sample. We attribute the 3.9 ppm peak in the preconditioned sample to isolated silanols on the silica surface, [46] however, an additional contribution to this resonance may be the rapid exchange of water with the silanols.[47] The peak at 4.3 ppm is a new peak that is broader due to overlap with the 3.9 ppm peak present in both samples. As with the preconditioned sample, the additional waters due to hydration of the Sc in the Sc-CA-SBA sample, are also likely in rapid exchange with the surface.[47] We assign the remaining chemical shifts of the Sc-CA-SBA ^{1}H spectrum based on a ring opened molecule. The resonances of the $-CH_2$ protons adjacent to the nitrogen and farther from the nitrogen are expected to be δ_H = 3-4 ppm and δ_H =0.5-2.5 ppm, respectively. Protons on the surface silanols are expected to have a shift of δ_H = 5-6.5 ppm.

In order to determine the association of the proton species with the sorbed Sc we performed $^{1}H\{^{45}Sc\}$ TRAPDOR NMR spectroscopy on the Sc-CA-SBA sample (Figure 10). The experiment proceeds by first collecting a ^{1}H spin echo 'control' spectrum (Figure 10a) that contains the unmodified intensity of all the ^{1}H species present in the sample. This 'control' spectrum is compared to that of the $^{1}H\{^{45}Sc\}$ TRAPDOR experiment (Figure 10b) that presents a loss in signal for all ^{1}H species that are coupled to ^{45}Sc in the sample. This comparison allows us to determine which protons in the solid are associated with the Sc. We observe a decrease in the intensity of the proton resonances from δ_H = 4.3-7.5 ppm as well as that at δ_H = 4.0 ppm in the TRAPDOR spectrum compared to the control. This result indicates that the Sc is correlated strongly with the surface silanols and the water molecules on the Sc molecule, further confirming their presence in the inner sphere of the Sc atom. Based on the structure of the ligand, the metal cation can only coordinate to the carbonyl oxygens. In this conformation, the next nearest ligand proton would reside at a minimum of about 3 Å from the Sc, which is too distant for the correlations observed in this TRAPDOR experiment.

The results of the TRAPDOR experiment only provide information that the Sc is interacting with the surface of the CA-SBA, and further experiments utilizing ^{1}H DQ correlation experiments can be used to further constrain the structure of the coordinating ligand and to determine if it interacts with the surface silanol protons. These results produce a map of the through-space correlations between proton species (Figure 11). At the short mixing time used, the chemical shifts in the DQ dimension occur at the linear combination of the single quantum chemical shifts, and represent only the closest associations between the two ^{1}H species.

The results clearly show strong associations between the $-CH_2$ groups on the chains but additional contours in the DQ dimension at 13.2 and 8.3 ppm reveal unique interactions of the amide and silanol functional groups, respectively. The DQ correlation at 13.2 ppm results from a correlation between the amide and its next adjacent proton at δ_H = 9.5 ppm and δ_H = 3.7 ppm, respectively. This result illustrates that for such correlations to occur these protons must be in close association (< 3.5 Å)[48] with one another. The DQ shift of δ_H = 8.3 ppm results from a close association between the protons represented by SQ shifts of of δ_H = 6.7 ppm and δ_H = 1.5 ppm. We assign this correlation to that between the surface silanols (6.7 ppm) and a ligand $-CH_2$ group

δ_H = 1.5 ppm, indicating that the ring opened ligand is bent towards the surface near the silanols, therefore also interacting with the Sc associated with the surface. Similar ligand interactions with a silica surface were previously observed with molecules terminating in trimethylamine.[47]

Based on the combined results from the SP/MAS, TRAPDOR, and DQ correlation experiment, we can propose a mechanism of Sc(III) interaction with the CA-SBA material. The Sc(III) appears to be simultaneously coordinating with the silanols on the SBA-15 surface and the carbonyls of the CA ligand . Based on the bidentate CA ligand occupying two sites on the coordination sphere of the Sc, and the silanols occupying two to three additional sites, there are most likely 2-3 waters in the inner coordination sphere of each Sc ion. The width of the ^{45}Sc SP/MAS resonance, the decrease in proton intensity at δ_H = 4.3-7.5 ppm and δ_H = 4 ppm in the TRAPDOR experiment, and the correlation between the silanol protons and the ligand $-CH_2$ protons in the DQ experiment combine to support that Sc(III) is coordinated with the ligand, silanols, and water molecules simultaneously.

A desorption experiment on the Sc-CA-SBA sample analogous to that performed on the Al-CA-SBA sample was carried out. A ^{45}Sc SP/MAS NMR spectrum was collected on the desorbed sample (d-Sc-CA-SBA, Figure 12b) and no change was observed relative to that of the Sc-CA-SBA (Figure 12a). We believe that this is because the Sc is already hydrolyzed during the initial sorption to the CA-SBA at pH 3. Above pH 2, hydrolysis of Sc has been observed, and at the concentrations of Sc used in this experiment, precipitation of ScOOH (s) is expected above pH 3.8.[49] However, based on the results of the ^{45}Sc spectrum, it is clear that there is still a substantial amount of Sc if not all of it remaining on the CA-SBA. Based on this result, within the timescale of this desorption experiment, Sc interactions with the ligand and the silanols are favored over precipitation.

DISCUSSION

These results indicate the CA functionalized SBA-15, is not completely stable in aqueous environments and that even in the presence of dilute (pH 3) nitric acid significant degradation of the ligand occurs. The results from the ^{13}C NMR indicate opening of the seven-membered ring on the ligands that remain attached to the silica. This mechanism allows the ligand to obtain a less sterically-hindered conformation for complexing metals. However,

the resulting ligand may then be susceptible to further acid degradation and the rate of diffusion of metals through the pores may decrease if the chain is long enough to clog pores. We also observed that occasionally complete detachment of the ligand can occur at the silane anchor on the silica surface, as evident by the ^{29}Si spectra. However, this partial retention of the ligand on the surface allows us to postulate the coordination environment of the metal complex. The observed ligand degradation in pH 3 nitric acid suggests that it is important to examine the characteristics of functionalized materials both before and after contact with acid as the actual pre-conditioned surface that contacts the metal may be different than the pristine material.

The behavior of Al and Sc on the CA-SBA and on the bare SBA differed in their coordination. Al(III) showed two different types of coordination when contacted with the CA-SBA, however, only one type of coordination on the bare SBA-15. This is indicative that one of the two sites present on the functionalized material is the Al(III) bound to the silica surface and the other interacted with the ligand. The Sc(III), however, primarily binds with a coordination number of seven both for the bare SBA-15 and the functionalized SBA-15. The functionalized sample, however, has a broader ^{45}Sc peak which we attribute to a more disordered structure caused by Sc coordination with the ligand. We confirmed that the Sc was complexing with the surface silanols and water molecules using $^{1}H\{^{45}Sc\}$ TRAPDOR NMR spectroscopy supported by a ^{1}H DQ correlation experiment. Through the desorption experiment with Al (III) on CA functionalized SBA-15, we determined that Al can be easily desorbed from the functionalized silica. The ability to desorb a species is important for any material that will be used as an extraction chromatography material. Unlike Al however, Sc could not be desorbed from CA-SBA under the same conditions. This means that under these conditions, if Al and Sc were both sorbed to CA-SBA, Al could be selectively removed, isolating Al from Sc.

In the absence of the detailed characterization we have presented macroscopic batch metal sorption experiments to functionalized solids cannot differentiate between metal sorbed to ligand sites or residual surface sites. The difference between an interaction with the surface versus with the ligand, however, can have major implications for the efficacy of the materials in either chromatography or catalysis applications. In the case of the CA ligand that we are discussing here, the metal interacts with the ligand via the carbonyls in a

coordination complex. If, however, the cations sorb to the surface, they either form ionic bonds with deprotonated silanols or interact via Van der Waals forces with the lone pairs on the silanol oxygen. The strength of these interactions cannot be postulated based on the results presented here but, the difference will likely affect a potential separation or catalyst application. Here we have shown that these cations can form multiple types of complexes with a material, and it likely that each complex will have different stability constants and, in turn, will behave like multiple distinct species in a single separation. At low pH values, metal-silanol interactions are often assumed to be minimal due to the metal speciation and protonated state of the surface. We see from the results presented here that these interactions cannot be ignored as they are a predominant mechanism in the system.

Multinuclear solid-state NMR provided unique insights into the interaction of metal nuclei with an organically modified silica surface. Based on these results, however, we also determined that the CA ligand may not be the most suitable for the desired applications. Beyond the immediately problematic issue of ligand degradation, the observation that the Sc(III) and Al(III) interact with both the silica surface and the ligand is also problematic because this limits our ability to tune the material selectivity via ligand characteristics. Ideally, the organically-modified silica would have a ligand that forms a strong enough complex with the metal ion that the interactions with the silica surface are negligible. Future work towards improving upon this material will incorporate ligands that complex the metal more strongly and are less susceptible to acid hydrolysis.

CONCLUSION

Al(III) and Sc(III) sorb to N-[5-(trimethoxysilyl)-2-aza-1-oxopentyl]caprolactam functionalized mesoporous silica via interactions with both the surface and the ligand. The 7-membered ring opens during the acid pre-conditioning, making it a less sterically hindered molecule. By probing not only the metal nuclei, but also carbon from the ligand, and silicon from the surface, we obtained a better understanding of how metals complex to this functionalized silica. While Al(III) and Sc(III) interact with the surface and the ligand, Al changes coordination number based on whether it is complexing with the ligand, while Sc maintains the same overall coordination number in both cases. While understanding the quantity of metals sorbed to these materials is important, we

364 must also examine the binding mechanisms and fundamental chemistry to most effectively develop new
365 materials. NMR spectroscopy has proved to be a useful tool for studying these mechanisms.

366

367 **ACKNOWLEDGEMENTS**
368
369 The authors would like to thank Professor A. Katz of the University of California, Berkeley for the TGA
370 measurements. This work was supported by the National Nuclear Security Administration (NNSA) under the
371 Stewardship Science Academic Alliance Program, award number DE-NA0001978 and by the Subsurface
372 Biogeochemical Research Program of the U.S. Department of Energy's Office of Biological and Environmental
373 Research. This work was performed under the auspices of the U.S. Department of Energy by Lawrence
374 Livermore National Laboratory under Contract DE-AC52-07NA27344. J.S. is supported by a DOE NNSA
375 Stewardship Science Graduate Fellowship under Contract No. DE-FC52-08NA28752.

FIGURES

Figure 1. a) N-[5-(trimethoxysilyl)-2-aza-1-oxopentyl]caprolactam grafted to silica and b) ring-opened structure occurring after contact with pH 3 nitric acid.

Figure 2. $^{29}Si\{^{1}H\}$ CP/MAS NMR spectra for CA functionalized SBA-15 a) pristine solid (CA-SBA) and b) pre-conditioned solid (p-CA-SBA). The resonances for the bulk silicon atoms are the Q peaks (Q^2, Q^3, and Q^4 have shifts of δ_{Si} =-93, -97, and -107 ppm, respectively) and for the surface silicon atoms are the T peaks (T^1, T^2, and T^3 have shifts of δ_{Si} =-51, -58, and -66 ppm, respectively).

Figure 3. $^{13}C\{^{1}H\}$ CP/MAS NMR spectra for CA functionalized SBA-15 a) pristine solid (CA-SBA) and b) pre-conditioned solid (p-CA-SBA). Dashed line highlights the 48 ppm resonance in the CA-SBA spectrum that is nearly absent in the p-CA-SBA spectrum, indicating ring-opening.

Figure 4. ^{27}Al SP/MAS NMR spectra of solids from Al sorption to a) bare SBA-15 (Al-SBA) and b) CA functionalized SBA-15 (Al-CA-SBA).

Figure 5. ^{45}Sc SP/MAS NMR spectra of solids from a) Sc sorption to bare SBA-15 (Sc-SBA) and b) CA functionalized SBA-15 (Sc-CA-SBA) collected on 300 MHz spectrometer. The chemical shifts for 6, 7, and 8-coordinated Sc occur in the ranges of δ_{Sc}=100 to 160 ppm, δ_{Sc} = 10 to 70 ppm, and δ_{Sc} =-10 to -50 ppm, respectively.[28]

Figure 6. $^{29}Si\{^{1}H\}$ CP/MAS NMR spectra for solids from a) pre-conditioned CA functionalized SBA-15 (p-CA-SBA), b) Al sorption to CA functionalized SBA-15 (Al-CA-SBA), and c) Sc sorption to CA functionalized SBA-15 (Sc-CA-SBA).

Figure 7. $^{13}C\{^{1}H\}$ CP/MAS NMR spectra for solids from a) pre-conditioned CA functionalized SBA-15 (p-CA-SBA), b) Al sorption to CA functionalized SBA-15 (Al-CA-SBA), and c) Sc sorption to CA functionalized SBA-15 (Sc-CA-SBA).

Figure 8. ^{27}Al SP/MAS NMR spectra of solids from Al sorption to CA functionalized SBA-15 a) before (Al-CA-SBA) and b) after contact with water for desorption (d-Al-CA-SBA).

Figure 9. ^{1}H SP/MAS NMR spectra of a) pre-conditioned CA functionalized SBA-15 (p-CA-SBA) and b) solid from Sc sorption to CA functionalized SBA-15 (Sc-CA-SBA). The dotted line highlights the H_2O peak present in the Sc-CA-SBA sample and absent in the p-CA-SBA sample. The dashed line highlights that the $-CH_2$ groups have not shifted.

Figure 10. $^{1}H\{^{45}Sc\}$ a) control (black) and b) TRAPDOR (red) spectra of solids from Sc sorption to CA functionalized SBA-15.

Figure 11. ^{1}H DQ correlation spectra of solids from Sc sorption to CA functionalized SBA-15. Positions of the 13.2 and 8.3 ppm DQ cross peaks are highlighted in red circles. ^{1}H chemical shift relative to external standard hydroxylapatite with the hydroxyl resonance at 0.2 ppm.

Figure 12. ^{45}Sc SP/MAS NMR spectra of solids from Sc sorption to CA functionalized SBA-15 a) before (Sc-CA-SBA) and b) after contact with water for desorption (d-Sc-CA-SBA). Spectra collected on 500 MHz spectrometer.

REFERENCES

1. J. Moreno, J. Iglesias, J. A. Melero, and D. C. Sherrington, *J. Mater. Chem.*, 2011, **21**, 6725.
2. S. Bhunia and S. Koner, *J. Porous Mater.*, 2010, **18**, 399–407.
3. M. U. Azmat, Y. Guo, Y. Guo, Y. Wang, and G. Lu, *J. Mol. Catal. A Chem.*, 2011, **336**, 42–50.
4. S. Tanaka, M. Tada, and Y. Iwasawa, *J. Catal.*, 2007, **245**, 173–183.
5. J. L. Rapp, Y. Huang, M. Natella, Y. Cai, V. S.-Y. Lin, and M. Pruski, *Solid State Nucl. Magn. Reson.*, 2009, **35**, 82–86.
6. A. Grünberg, X. Yeping, H. Breitzke, and G. Buntkowsky, *Chemistry*, 2010, **16**, 6993–8.
7. G. D. Zhao, D., Feng, J., Huo, Q., Melosh, N., Fredrickson, G.H., Chmelka, B.F., Stucky, *Science (80-.).*, 1998, **279**, 548–552.
8. P. Trens, M. L. Russell, L. Spjuth, M. J. Hudson, and J.-O. Liljenzin, *Ind. Eng. Chem. Res.*, 2002, **41**, 5220–5225.
9. Y. Sasaki, Y. Sugo, S. Suzuki, and T. Kimura, *Anal. Chim. Acta*, 2005, **543**, 31–37.
10. D. Das, S. A. Ansari, P. K. Mohapatra, G. Mary, K. Radhakrishnan, S. C. Tripathi, and V. K. Manchnada, *J. Radioanal. Nucl. Chem.*, 2011, **287**, 293–298.
11. M. M. R. Garcia, 2004.
12. B. Gannaz, M. R. Antonio, R. Chiarizia, C. Hill, and G. Cote, *Dalton Trans.*, 2006, 4553–62.
13. a. Sengupta, S. K. Thulasidas, V. C. Adya, P. K. Mohapatra, S. V. Godbole, and V. K. Manchanda, *J. Radioanal. Nucl. Chem.*, 2011, **292**, 1017–1023.
14. J. Broudic, O. Conocar, J. J. E. Moreau, D. Meyer, and M. W. C. Man, 1999, 2283–2285.
15. K. Van Hecke and G. Modolo, *J. Radioanal. Nucl. Chem.*, 2004, **261**, 269–275.
16. S. Bourg, J.-C. Broudic, O. Conocar, J. J. E. Moreau, D. Meyer, and M. Wong Chi Man, *Chem. Mater.*, 2001, **13**, 491–499.
17. R. D. Shannon, *Acta Crystallogr.*, 1976, **A32**, 751.
18. G. E. Fryxell, H. Wu, Y. Lin, W. J. Shaw, J. C. Birnbaum, J. C. Linehan, Z. Nie, K. Kemner, and S. Kelly, *J. Mater. Chem.*, 2004, **14**, 3356.
19. K. M. Feng, X., Fryxell, G.E., Wang, L.-Q., Kim, A.Y., Liu, J., Kemner, *Science (80-.).*, 1997, **276**, 923–926.
20. Y. Lin, S. K. Fiskum, W. Yantasee, H. Wu, S. V Mattigod, E. Vorpagel, G. E. Fryxell, K. N. Raymond, and J. Xu, *Environ. Sci. Technol.*, 2005, **39**, 1332–7.

21. T. G. Carter, W. Yantasee, T. Sangvanich, G. E. Fryxell, D. W. Johnson, and R. S. Addleman, *Chem. Commun. (Camb).*, 2008, 5583–5.

22. G. E. Fryxell, Y. Lin, S. Fiskum, J. C. Birnbaum, H. Wu, K. Kemner, and S. Kelly, *Environ. Sci. Technol.*, 2005, **39**, 1324–1331.

23. R. I. Nooney, M. Kalyanaraman, G. Kennedy, and E. J. Maginn, *Langmuir*, 2001, **17**, 528–533.

24. H. E. Mason, R. S. Maxwell, and S. A. Carroll, *Geochim. Cosmochim. Acta*, 2011, **75**, 6080–6093.

25. J. R. Houston, J. L. Herberg, R. S. Maxwell, and S. A. Carroll, *Geochim. Cosmochim. Acta*, 2008, **72**, 3326–3337.

26. S. Sen and J. F. Stebbins, *J. Non. Cryst. Solids*, 1995, **188**, 54–62.

27. C. Merkens, O. Pecher, F. Steuber, S. Eisenhut, A. Görne, F. Haarmann, and U. Englert, *Zeitschrift für Anorg. und Allg. Chemie*, 2013, **639**, 340–346.

28. N. Kim, C.-H. Hsieh, and J. F. Stebbins, *Chem. Mater.*, 2006, **18**, 3855–3859.

29. A. J. Rossini and R. W. Schurko, *J. Am. Chem. Soc.*, 2006, **128**, 10391–402.

30. D. Rehder and K. Hink, *Inorganica Chim. Acta*, 1989, **158**, 265–271.

31. A. Katiyar, S. Yadav, P. G. Smirniotis, and N. G. Pinto, *J. Chromatogr. A*, 2006, **1122**, 13–20.

32. C. P. Grey, W. S. Veeman, and A. J. Vega, *J. Chem. Phys.*, 1993, **98**, 7711.

33. C. P. Grey and W. S. Veeman, *Chem. Phys. Lett.*, 1992, **192**, 379–385.

34. W. Sommer, J. Gottwald, D. E. Demco, and H. W. Spiess, *J. Magn. Reson.*, 1995, **113**, 131–134.

35. M. Feike, D. E. Demco, R. Graf, J. Gottwald, S. Hafner, and H. W. Spiess, *J. Magn. Reson.*, 1996, **122**, 214–221.

36. J. P. Yesinowski and H. Eckert, *J. Am. Chem. Soc.*, 1987, **109**, 6274–6282.

37. M. Etienne and A. Walcarius, *Talanta*, 2003, **59**, 1173–88.

38. N. Bibent, T. Charpentier, S. Devautour-Vinot, A. Mehdi, P. Gaveau, F. Henn, and G. Silly, *Eur. J. Inorg. Chem.*, 2013, 2350–2361.

39. K. J. D. MacKenzie and M. E. Smith, *Multinuclear Solid-State NMR of Inorganic Materials*, Pergamon, New York, 2002.

40. S. A. Cotton, *Comments Inorg. Chem.*, 1999, **21**, 165–173.

41. P. Lindqvist-Reis, I. Persson, and M. Sandström, *Dalton Trans.*, 2006, 3868–78.

42. M. Katkova, T. Balashova, A. P. Pushkarev, I. Y. Ilyin, G. K. Fukin, E. V. Baranov, S. Y. Ketkov, and M. N. Bochkarev, *Dalton*, 2011, **40**, 7713–7717.

43. J. Narbutt, M. Czerwinski, and J. Krejzler, *Eur. J. Inorg. Chem.*, 2001, 3187–3197.

44. J. D. Kubicki, D. Sykes, and S. E. Apitz, *J. Phys. Chem. A*, 1999, **103**, 903–915.

45. P. Jain, H. J. Avila-Paredes, C. Gapuz, S. Sen, and S. Kim, *J. Phys. Chem. C*, 2009, **113**, 6553–6560.

46. C. C. Liu and G. E. Maciel, 1996, **118**, 5103–5119.

47. J. Trébosc, J. W. Wiench, S. Huh, V. S.-Y. Lin, and M. Pruski, *J. Am. Chem. Soc.*, 2005, **127**, 3057–68.

48. S. Pawsey, M. McCormick, S. De Paul, R. Graf, Y. S. Lee, L. Reven, and H. W. Spiess, *J. Am. Chem. Soc.*, 2003, **125**, 4174–84.

49. S. A. Wood and I. M. Samson, *Ore Geol. Rev.*, 2006, **28**, 57–102.

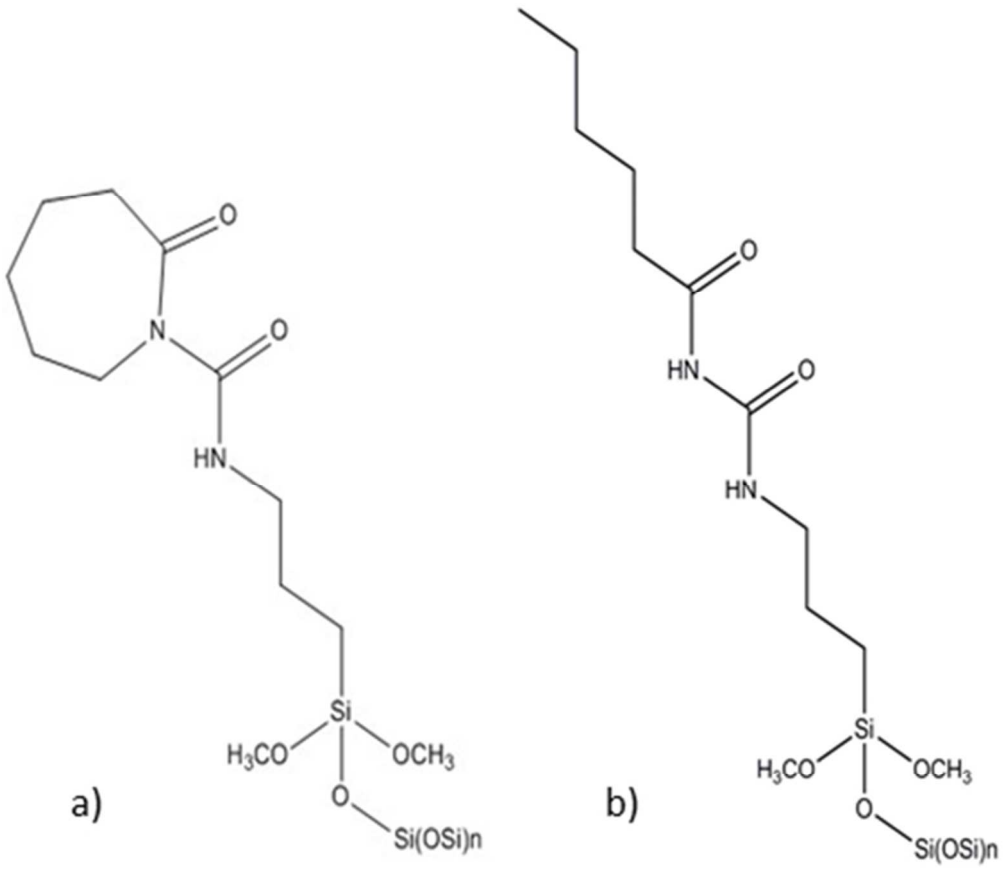

66x57mm (300 x 300 DPI)

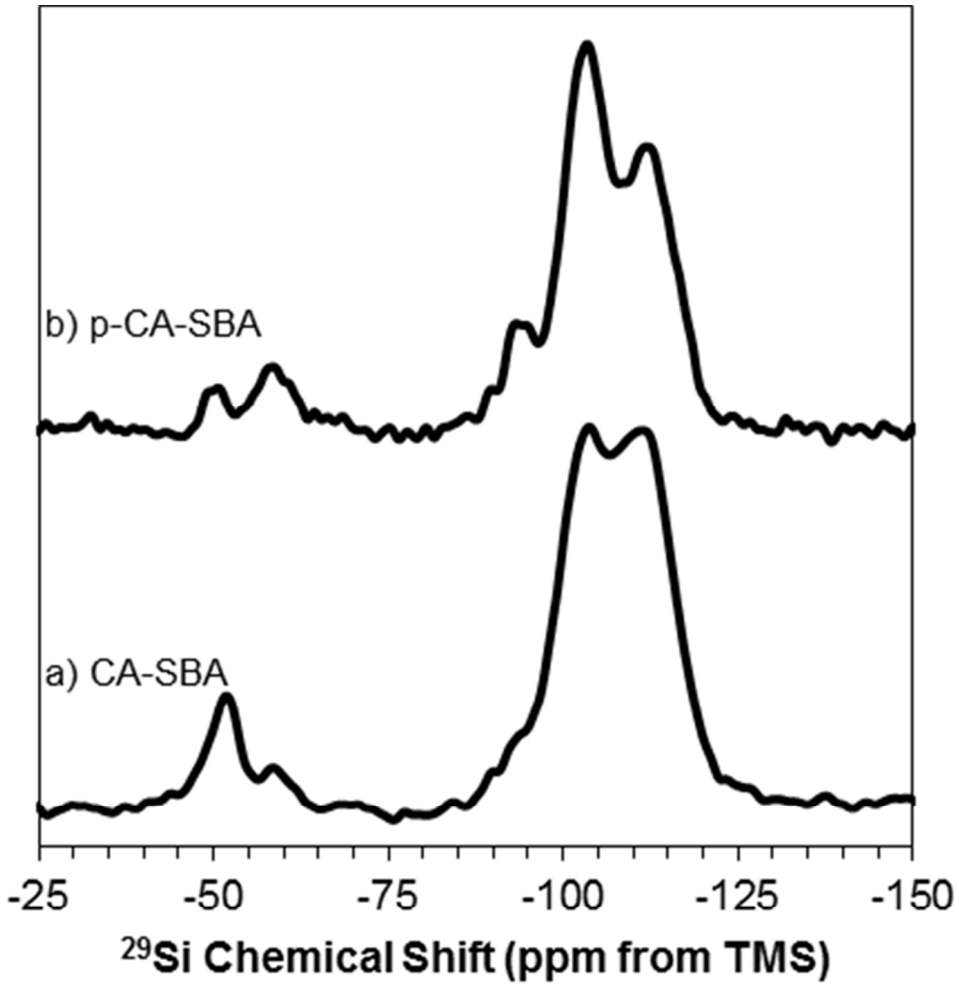

76x76mm (300 x 300 DPI)

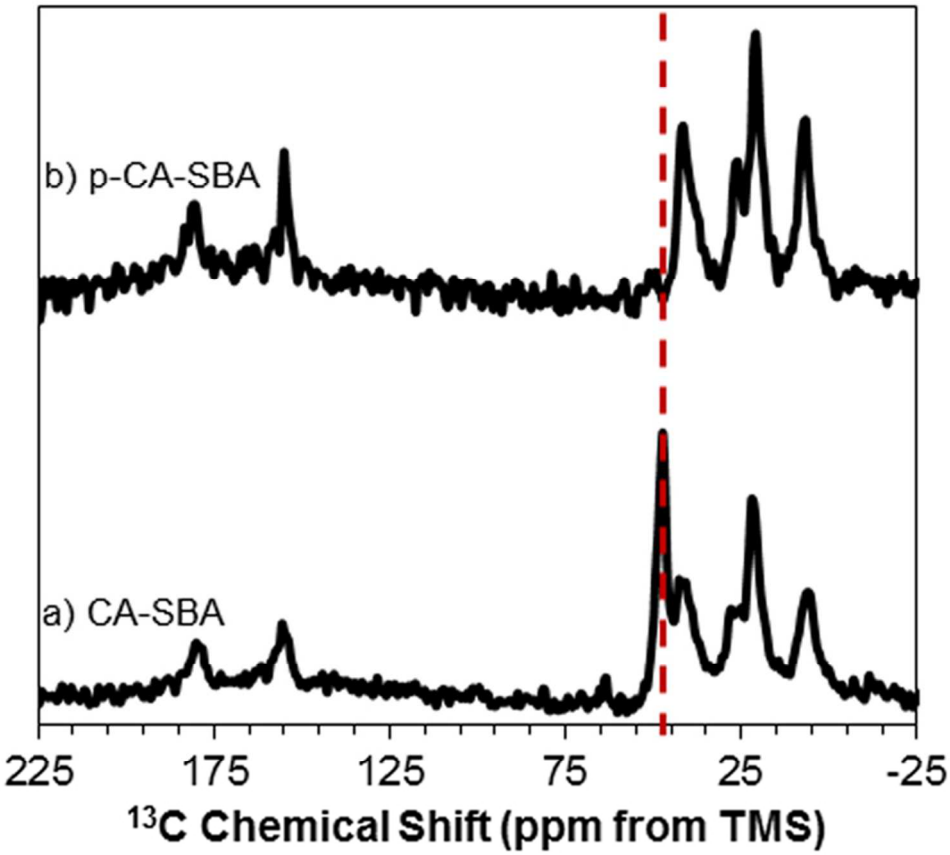

65x56mm (300 x 300 DPI)

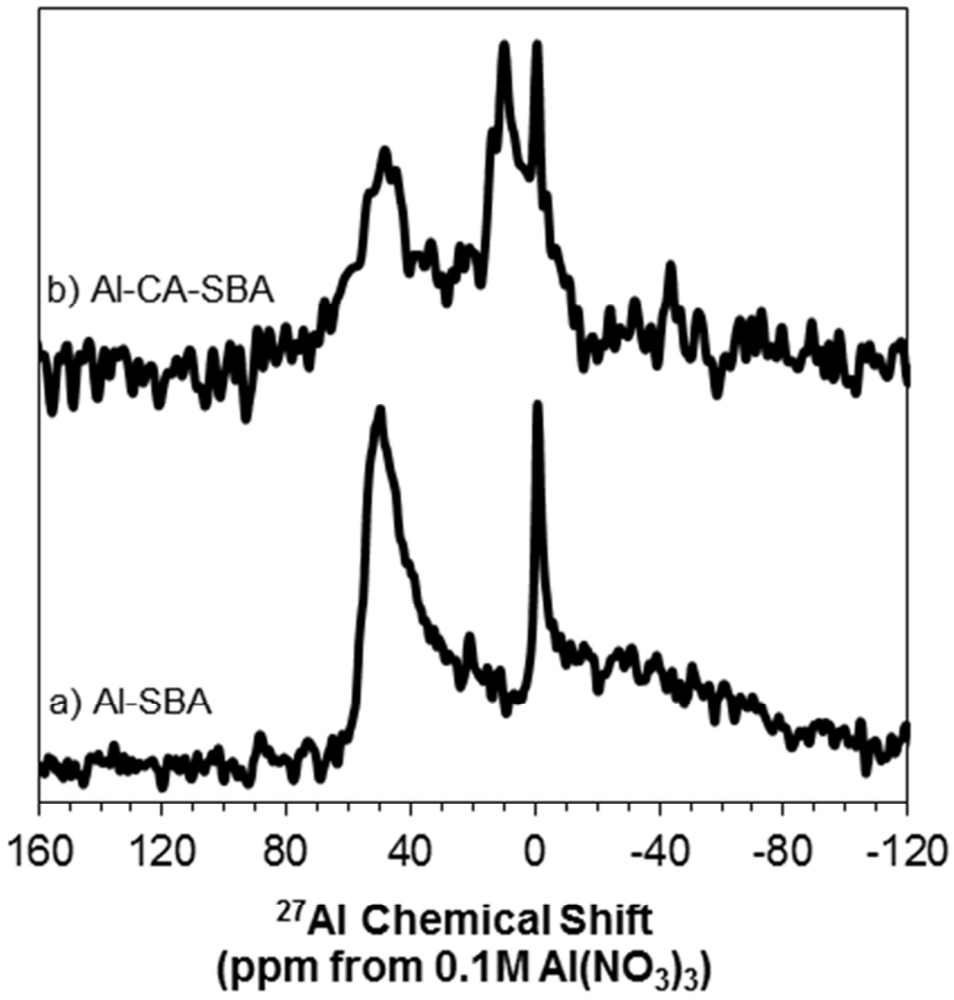

76x76mm (300 x 300 DPI)

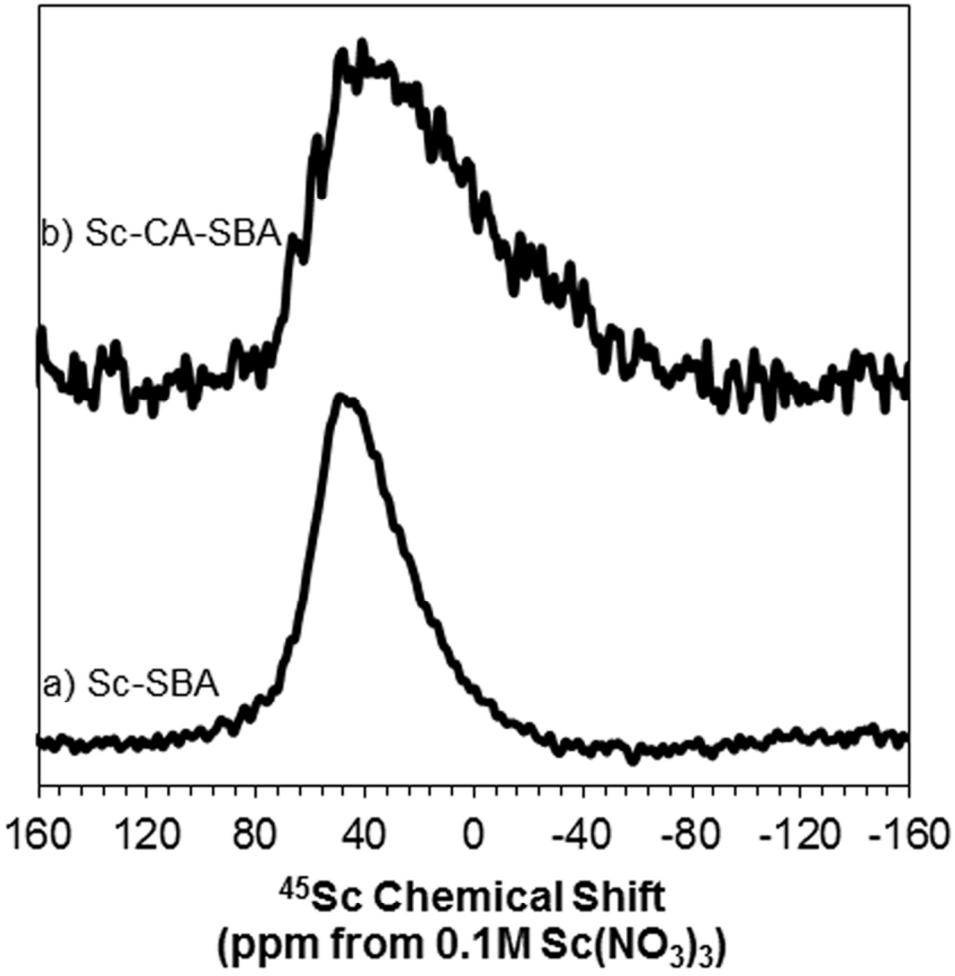

76x76mm (300 x 300 DPI)

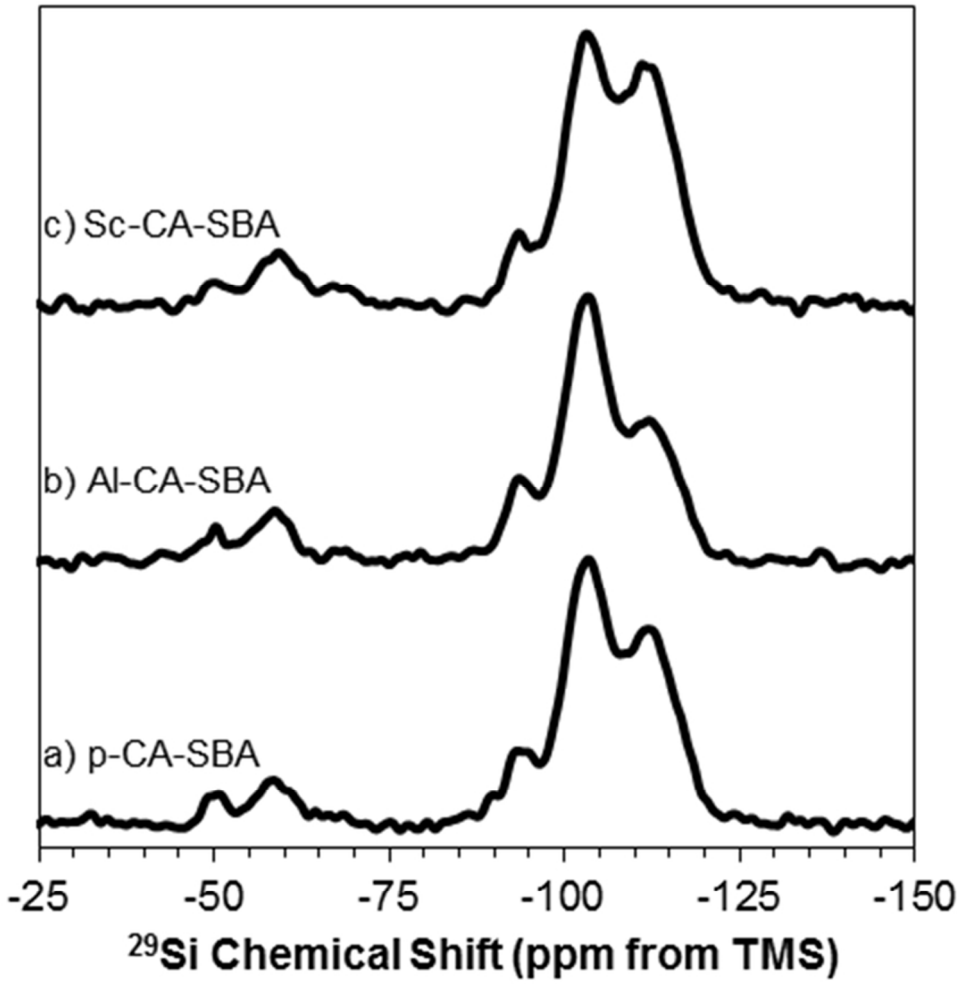

76x77mm (300 x 300 DPI)

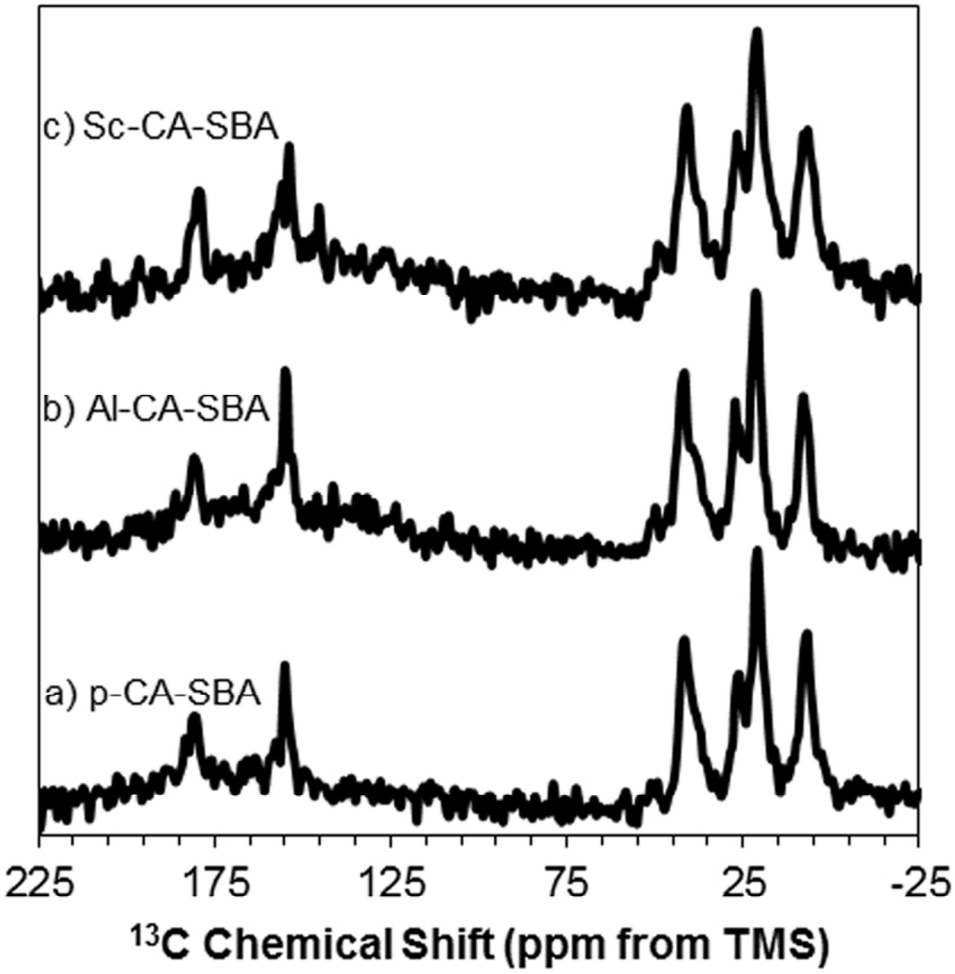

76x76mm (300 x 300 DPI)

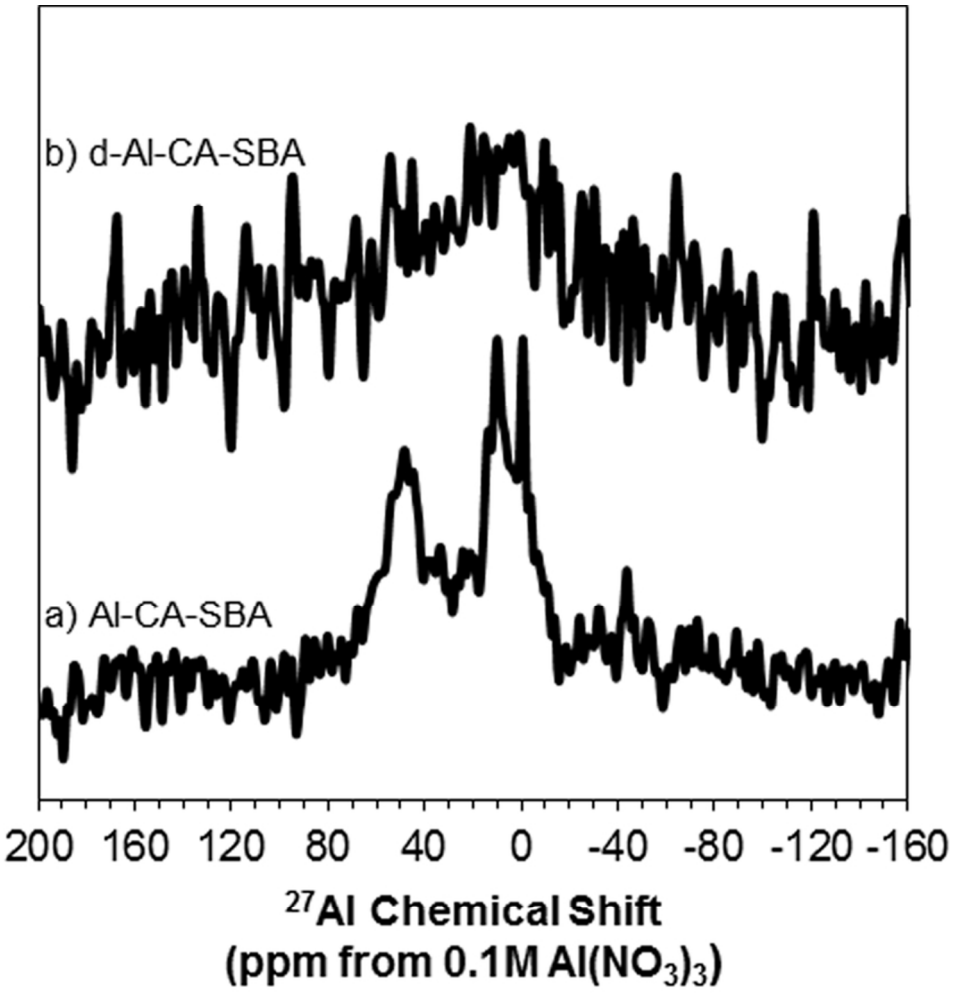

76x76mm (300 x 300 DPI)

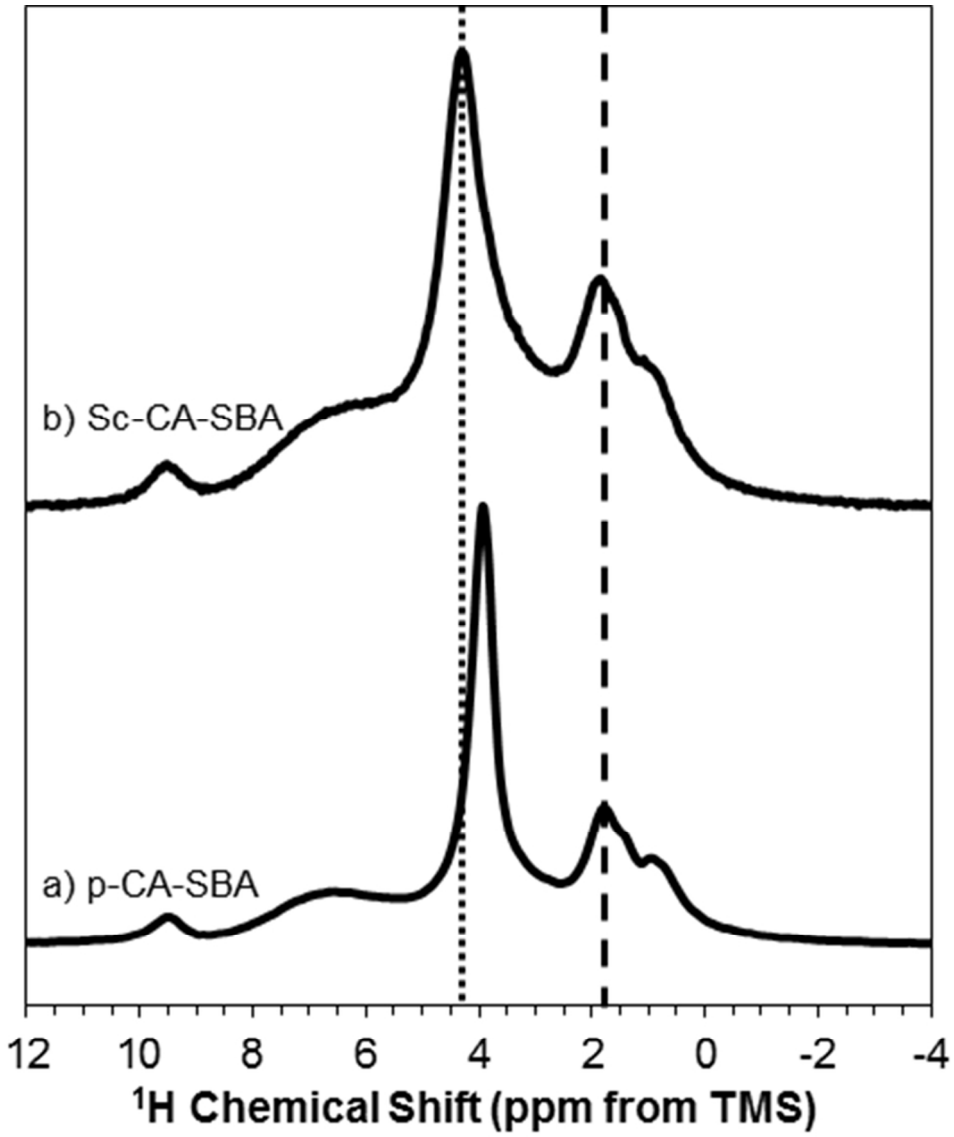

86x97mm (300 x 300 DPI)

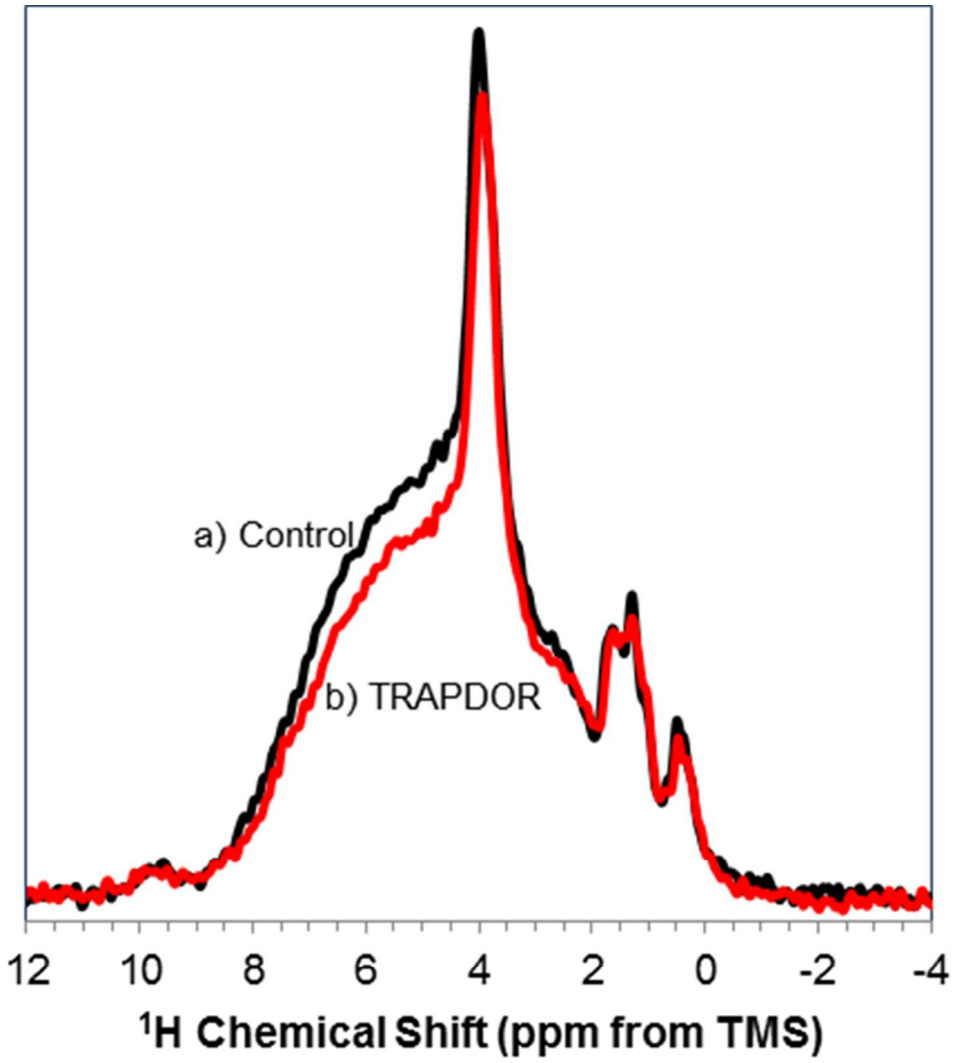

81x86mm (300 x 300 DPI)

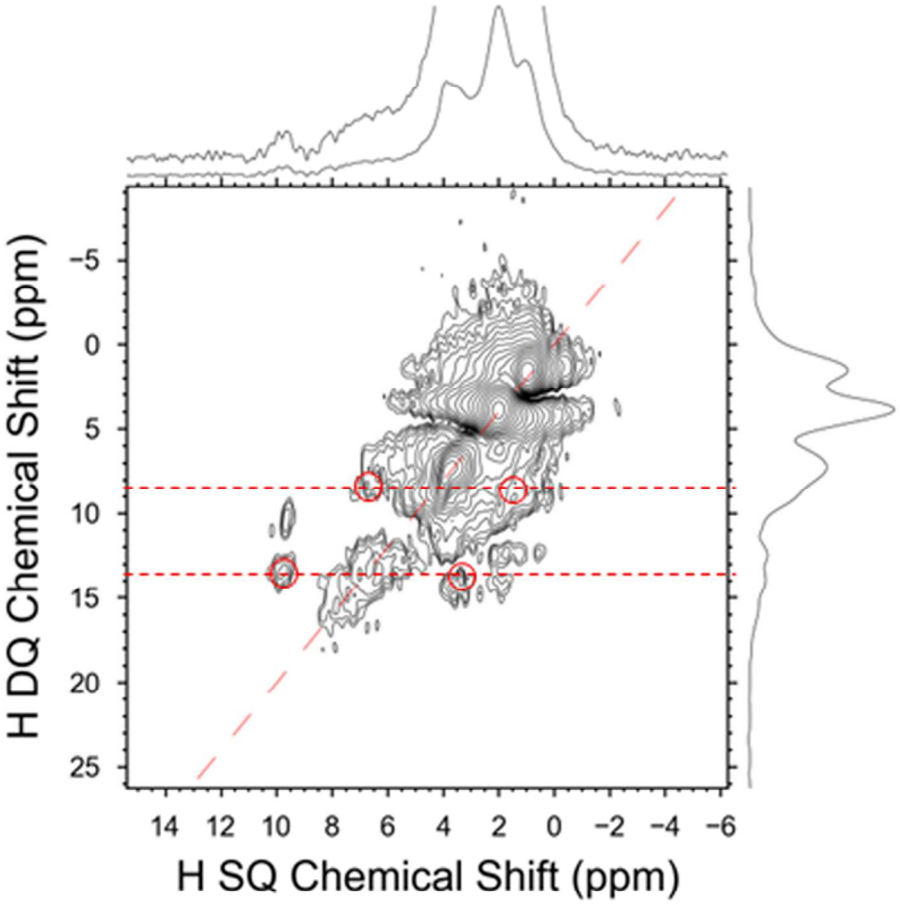

76x76mm (300 x 300 DPI)

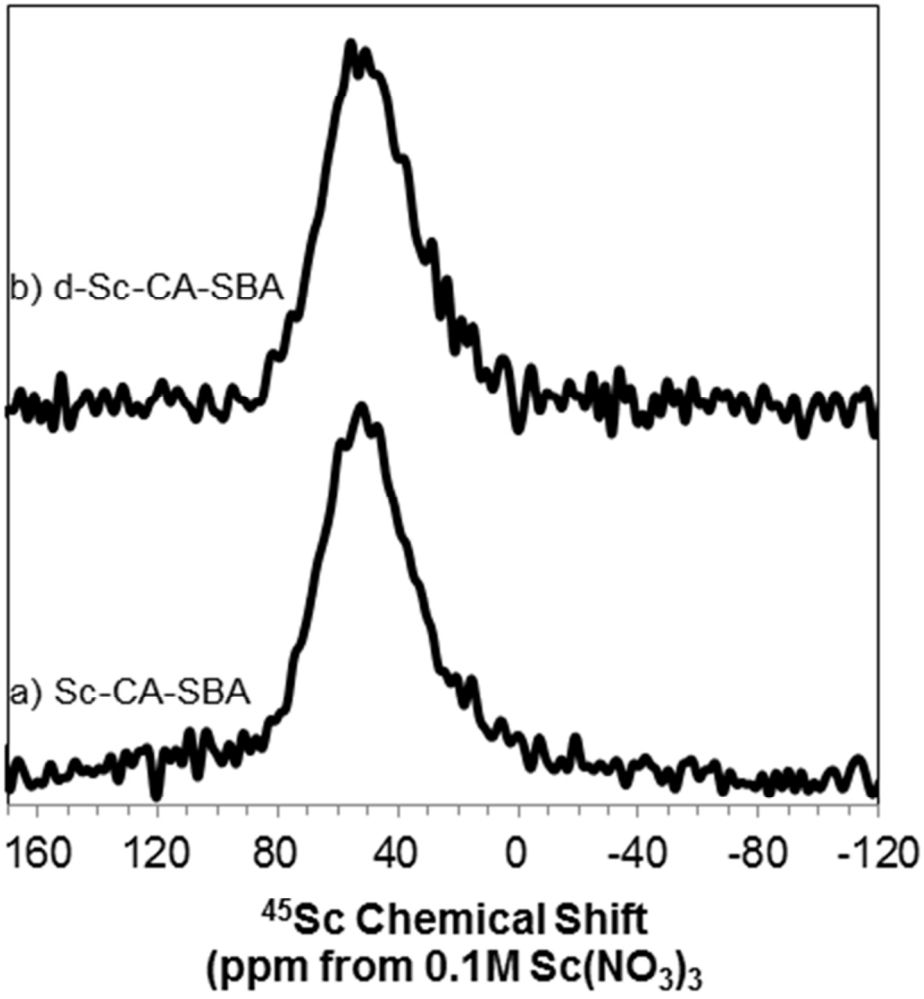

76x76mm (300 x 300 DPI)